

Time Dependent and Cycle Dependent Behaviour of Sintered Silicon Carbide and Alumina Ceramics

A.T. YOKOBORI, JR.* , T. ADACHI* , T. YOKOBORI** ,
H. ABE*** , J. NAKAYAMA*** , H. TAKAHASHI***
and H. MIYATA†

*Department of Mechanical Engineering II, Tohoku University,
Sendai, Japan

**Tokai University, Sagami, Kanagawa, Japan

***Research Laboratory, Asahi Glass Co., Ltd., Yokohama, Japan

†Mechanical Engineering Research Laboratory, Hitachi, Ltd.,
Tsuchiura, Japan

ABSTRACT

Stress rate dependence of strength, static fatigue and cyclic fatigue were studied for sintered silicon carbide and alumina ceramics. The strength of silicon carbide decreases with increase of stress rate and is not affected by time-dependent mechanism or cycle-dependent mechanism. Fracture occurs at constant strain. On the other hand, the strength of alumina ceramics increases with increase of stress rate and is affected by time-dependent mechanism in the lower frequency range and by cycle-dependent mechanism at higher frequencies. The transition region from time dependent control to cycle dependent control is discussed.

KEYWORDS

Ceramics; sintered silicon carbide; alumina ceramics; stress rate dependence; static fatigue; cyclic fatigue; time-dependent mechanism; cycle-dependent mechanism

1. INTRODUCTION

The fatigue life of ceramics is influenced by the grown-in defects. These defects may be considered as origins of most of the fatigue failures (Tanaka and Sakaida 1987). If such defects were not contained, the fatigue life would be much longer and the scatter of the data would be smaller (Ohara, Yokobori, Jr., Nakaguchi, Aizawa and Adachi 1987). The grown-in defects, which are the origins of fatigue cracks, do not result in a decrease of the static strength and can not be detected by proof test (Ohara, Yokobori, Jr., and Nojiri 1986). This is the reason why it is difficult to estimate fatigue life accurately.

When the e defects grow as the fatigue crack and the stress intensity factor amount to the fracture toughness, fracture occurs. (Ohara, Yokobori,

Jr., Nakaguchi, Aizawa and Adachi 1987). Although several papers discussed the cycle and time-dependent mechanism of fatigue crack growth for ceramics materials (Krohn and Hasselman 1972; Guiu 1978; Daushardt, Yu and Ritchie 1987; Evans and Linzer 1976), there are not so many works which concern systematic and comparative studies on the problem whether fatigue crack growth of ceramics is controlled by the number of load cycles or by time dependent process including various types of experimental estimation method. The present studies have been carried out on the line of this consideration. That is, in order to make clear these problems described above, the stress rate dependence of the strength, the static fatigue life and the cyclic fatigue life were studied for sintered silicon carbide and alumina ceramics ($Al_2O_3 \cdot SiO_2$), and these mechanical behaviours for both ceramics were compared. Furthermore, the transition region from time-dependent control to cycle-dependent control was investigated for cyclic fatigue tests on alumina ceramics.

2. MATERIALS, EXPERIMENTAL APPARATUS AND PROCEDURE

2.1 Materials

Materials used were sintered silicon carbide (SiC) and polycrystalline alumina ($Al_2O_3 \cdot SiO_2$). The specimen of each material was flat plate (70mm×4mm×1.5mm). These specimens were ground and polished. All experiments were carried out at room temperature and ambient atmosphere.

2.2 Test Method for Stress Rate Dependence of Fracture Strength

The experiments were carried out by two different methods. The first set of experiments were carried out by a four-point bending method using an Autograph testing machine at four different cross head speeds (0.1, 0.5, 5, 25 mm/min), to measure the stress rate dependence of bending strength. The major span was 30 mm and the minor span was 10 mm. Young's modulus E was calculated by using the following equation:

$$E = \frac{2s^2 + 2st - t^2}{12h} \cdot \frac{\sigma}{\delta} \quad (1)$$

where σ is the bending strength, δ is the deflection at fracture, h is specimen thickness, s is major span and t is minor span. The second set of experiments were by a quasi-static loading method, that is, load was increased step by step as shown in Fig.1. Load increment was 1 kgf and at each load level the load was held for about 10 sec. In this second test method, the effect of time-dependent mechanism on the strength may be obtained by varying the holding time of the load. Load was applied in four-point bending with major and minor spans of 40 and 10 mm.

2.3 Static Fatigue Test

The test was carried out using the same testing machine as that used in the quasi-static loading experiments described in §2.2. The specimens were loaded by four-point bending. For this test, the fatigue life time was

recorded by a timer which was connected to the machine. If the specimen did not fracture in 10^6 sec, then the test was stopped.

2.4 Cyclic Fatigue Test

The experiments were carried out by a four-point bending method using an Autograph fatigue testing machine. In this test, triangular wave form of load, with load ratio (Pmin/Pmax) R=0, was applied to the specimens. The applied load frequency ranged from 10^{-3} to 10^0 Hz. For comparison, the experimental results of fatigue life at 660Hz are referred to herein. These data were obtained by a resonance vibration fatigue test (Ohara, Yokobori, Jr., Nakaguchi, Aizawa and Adachi 1987).

2.5 Young's Modulus Measured by Resonance Vibration Method

The experimental devices are schematically shown in Fig.2. Sine wave generated by an oscillator was amplified to drive a transducer which consisted of an electric magnet. The sinusoidal stress was applied indirectly to the specimen one side of which was fixed. The thin steel plate was adhered to the other side. Frequency of the oscillator was adjusted to resonate the specimen at the first natural frequency. The resonance frequency was measured by a frequency counter. The Young's modulus is given by the equation:

$$E = \frac{48\pi^2}{(\xi l)^4} \left(\frac{l}{h}\right)^3 \rho h l f^2 \quad (2)$$

where f is the first natural frequency, b is specimen width, h is specimen thickness, l is specimen length, ρ is specimen density and ξl is the solution of the following equation:

$$1 + \cos \xi l \cos \xi l + \alpha \xi l (\cos \xi l \sinh \xi l - \sin \xi l \cosh \xi l) = 0 \quad (3)$$

where $\alpha = m/\rho b h l$, m is mass of the thin steel plate. By this method Young's modulus can be measured accurately. Young's modulus obtained was compared with that measured by the four-point bending method.

3. EXPERIMENTAL RESULTS

3.1 Sintered Silicon Carbide

3.1.1 Stress Rate Dependence of Bending Strength Experimental results of the stress rate ($\dot{\sigma}$) dependence of the bending strength are shown in Fig.3. For stressing rates up to $\dot{\sigma} = 15$ MPa/sec, the strength increases with increasing stress rate and at $\dot{\sigma} = 15$ MPa/sec, reaches a maximum value and then decreases with further increase of stress rate. This results coincide with other experimental results (Popp and Pabst 1981), although the authors did not discuss in that paper. The bending strength measured in a quasi-static loading test is also shown in Fig.3. The strength obtained by this quasi-static loading test is nearly equal to that at $\dot{\sigma} = 1.5$ MPa/sec. Thus, the

strength does not decrease due to the time effect involved in such static loading, that is, time-dependent mechanism does not play a role. Young's modulus and the deflection at fracture are shown in Figs. 4 and 5, respectively. The stress rate dependence of Young's modulus is similar to that of the bending strength, and at $\dot{\sigma}=15\text{MPa/sec}$, Young's modulus takes maximum value. But the deflection at fracture is independent of the stress rate and takes almost constant value. Consequently, fracture of sintered silicon carbide material is considered to occur at constant strain.

3.1.2 Static Fatigue and Cyclic Fatigue Characteristics The experimental results obtained by the static fatigue test are shown in Fig.6. The applied stress level is larger than the fracture stress under quasi-static loading test. However most of the specimens fractured abruptly when stress was applied, or did not fracture even after a time of 10^6 sec; a few specimens fractured after elapse of finite time. Therefore, fracture life of SiC under static fatigue condition is not affected by time-dependent processes. On the other hand, for a cyclic fatigue test, the effect of the number of cycles (cycle effect) can not be seen in fracture life (Fig.7). Only one specimen fractured within finite life. These results show that neither time nor the number of cycles have a dominant effect on the fracture life of silicon carbide. These results are in good agreement with those under high temperature condition (Fujita, Kawai, Takahashi, Abe and Nakayama 1985). Therefore, measurements of strength and fracture deflection under monotonic loading are adequate for practical application. Especially, since fracture deflection is independent of the applied loading rate, high strength durability under both static and cyclic fatigue conditions will be assured if deflection is controlled to be less than the critical fracture strain under monotonical load.

3.2 Alumina Ceramics

3.2.1 Stress Rate Dependence of Bending Strength The stress rate dependence of bending strength is shown in Fig.8. The strength increases with increase of the stress rate. On the other hand, the strength by a quasi-static loading method decreases remarkably. Therefore, the alumina ceramic is very sensitive to time-dependent mechanism as compared with silicon carbide. The stress rate dependence of Young's modulus and the deflection at fracture are shown in Figs.9 and 10. Both properties are approximately similar to that of the strength. From these results of silicon carbide and alumina ceramics, the comparison method between monotonical loading test and quasi-static loading method is shown to be convenient to show whether ceramics is affected sensitively by time-dependent process or not.

3.2.2 Static Fatigue Characteristics The experimental results on static fatigue test are shown in Fig.11. For alumina ceramics most of the specimens fractured within finite life. Thus fracture is controlled by time-dependent mechanism. The fracture life increases as the stress level becomes lower, and shows the tendency of saturation. Therefore, the static fatigue limit is suggested.

3.2.3 Cyclic Fatigue Characteristics The experimental results of cyclic fatigue test are shown in Fig.12. The fracture life increases as the

stress amplitude decreases. Cyclic fatigue limit appears to exist. But at each applied stress amplitude, the life increases as applied loading frequency increases. Thus, an effect of time-dependent mechanism is involved even under cyclic fatigue loading condition.

3.3 Characterization of Time Dependent and Cycle Dependent Nature of Fatigue Life with Respect to Applied Loading Frequency

In order to make clear whether the experimental results of alumina ceramics under cyclic fatigue test are time dependent only or the number of cycles dependent only, the results in a cyclic fatigue test were analysed by the estimation method as shown in Fig.13 (Yokobori Jr. *et al.*, 1986; Yokobori Jr. *et al.*, 1986; Yokobori Jr. *et al.*, 1986). When the logarithm of inverse of fatigue life, $1/t_f$, is parallel to the horizontal axis, that is, logarithm of frequency axis, fatigue life is considered as controlled by only time-dependent mechanism. On the other hand, when the logarithm of $1/t_f$ has the gradient of 45 degree against logarithm of frequency axis, fatigue life is considered as controlled by only the number of cycles (cycle) dependent mechanism. Cyclic fatigue life of alumina ceramics obtained by this estimation method is plotted against applied loading frequency as shown in Figs.14 and 15. From Figs.14 and 15, it can be seen that when applied loading amplitude is small (230MPa, Fig.14), the logarithm of inverse of fatigue life $1/t_f$ tends to saturate some constant value with decrease of frequency below $f < 10^{-1}\text{Hz}$. On the other hand, $1/t_f$ increases with increase of frequency with the gradient of 45 degree against frequency axis for $f > 10^{-1}\text{Hz}$, and takes minimum value at $5 \times 10^{-2}\text{Hz}$, which is the transition point from time-dependent mechanism only to cycle-dependent mechanism only. The fatigue life around this transition point is assumed to be controlled by both time-dependent and cycle-dependent mechanisms. When the applied loading amplitude becomes large (260MPa, Fig.15), the transition from time-dependent mechanism to cycle-dependent mechanism in $1/t_f$ characteristics occurs with monotonically changing trend. Nevertheless, with the decrease of the applied load amplitude, say, (230MPa, Fig.14), minimum point will appear within the transition range. It is interesting to note that these characteristics are similar to the corrosion fatigue of metals (Yokobori Jr., Yokobori, Kosumi and Takasu 1986), which suggests cyclic fatigue behaviour of alumina ceramics is at least apparently similar to metal corrosion fatigue behaviour. Furthermore it appears that the frequency of the transition point becomes large with increase of stress amplitude as shown in Figs.14 and 15, which show transition behaviour is affected by gross stress.

3.4 Discussion on Young's Modulus Measured by Resonance Vibration Test Method

Table 1 shows the experimental results on silicon carbide and alumina ceramics measured by resonance vibration method which is very accurate measurement of Young's modulus. The value of Young's modulus of both specimens are nearly similar to those calculated from measurements in a four-point bending test. Consequently, the value of Young's modulus obtained from measurements in a four-point bending method may be considered as accurate as by the resonance vibration test method.

4. CONSIDERATION AND DISCUSSION

For alumina ceramics, as is shown in §3.3 and Figs.14 and 15, when applied stress level becomes smaller, the transition point from time-dependent mechanism to cycle-dependent mechanism moves towards lower range of frequency, and transition behaviour is pronounced. Thus the effect of cycle-dependent mechanism is shown to be pronounced under lower stress condition. On the other hand, when applied stress level becomes higher, the transition point moves towards higher range of frequency and the effect of time-dependent mechanism becomes dominant.

It is to be noted that this characteristics appears quite similar as the relation between the fatigue crack growth rate and frequency for sintered silicon nitride (Kishimoto, Ueno and Kawamoto 1987) as shown in Fig.16. Since $1/t_f$ (the logarithm of inverse of fatigue life) and gross stress may be considered as corresponding to the fatigue crack growth rate da/dt and stress intensity factor, respectively, we can understand that alumina ceramics and sintered silicon nitride have similar time and cycle dependent trends with respect to frequency and applied stress level.

Although the fatigue failure mechanism for ceramics materials was discussed and was compared with metal materials, (Evans and Linzer 1976; Ewart and Suresh 1987), it is to be noted that in the present paper, the systematic and comparative studies of various types of tests methods, such as, monotonic, quasi-static, static fatigue and cyclic fatigue tests were carried out, and, moreover for the case of cyclic fatigue test the characteristics were studied over wide range of frequency. Note that as shown in Figs.14 and 15 the test was ranged to frequency of 660Hz.

5. CONCLUSION

- (1) The bending strength under static test of sintered silicon carbide increases, takes maximum value and then decreases with increase of the stress rate.
- (2) Sintered silicon carbide is not so much affected by time-dependent mechanism nor cycle-dependent mechanism but fractures at the constant strain. Therefore, endurance will be assured if strain is kept less than fracture strain under the monotonical applied load.
- (3) The time-dependent mechanism is dominant in the fracture life of alumina ceramics. Endurance limit appears to exist, not only under time dependent condition but also cycle dependent condition.
- (4) The fracture life of alumina ceramics under cyclic loading is controlled by time-dependent mechanism at low frequencies and controlled by cycle-dependent mechanism at higher frequencies. The transition of the mechanisms is controlled by applied load level in such way that cycle-dependent process will be more pronounced under smaller stress level, but time dependent process dominant under higher stress level. The transition frequency from time-dependent mechanism to cycle-dependent mechanism appears to increase with increase of applied load.

REFERENCES

Dauskardt, R.H., W. Yu and R.O. Ritchie (1987). Journal of the American Ceramic Society Vol.70, C248.

Evans, A.G. and M. Linzer (1976). International Journal of Fracture Vol.12, 217

Ewart, L. and S. Suresh (1987). Journal of Materials Science, Vol.22, 1173.

Fujita, H., M. Kawai, H. Takahashi, H. Abe and J. Nakayama (1985). Proceedings of Fourth International Symposium on the Fracture Mechanics of Ceramics, 1, Virginia Polytech. Inst. and State Univ.

Guiu, F. (1978). Journal of Materials Science, Vol.13, 1357.

Kishimoto, H., A. Ueno and H. Kawamoto (1987). Proceedings of the 32nd Japan National Symposium of Strength, Fracture and Fatigue, 61.

Krohn, D.A. and D.P.H. Hasselman (1972). Journal of the American Ceramic Society, Vol.55, 4, 208.

Ohara, H., A.T.Jr. Yokobori, M. Nakaguchi, Y. Aizawa and T. Adachi (1987). Journal of the Japanese Society for Strength and Fracture of Materials, Vol.23, 1, 1 (in Japanese).

Ohara, H., A.T.Jr. Yokobori and K. Nojiri (1987). Journal of the Ceramic Society of Japan, Vol.95, 1059.

Popp, G. and R.F. Pabst (1981). Metal Science, Vol.15, 130.

Tanaka, T. and A. Sakaida (1987). Transactions of the Japan Society of Mechanical Engineers Vol.53, 1566.

Yokobori, A.T.Jr., T. Kuriyama, Y. Kaji and T. Yokobori (1986). Journal of the Japanese Society for Strength and Fracture of Materials, Vol.21, 1 (in Japanese).

Yokobori, A.T.Jr., T. Yokobori, T. Kosumi and N. Takasu (1986). Corrosion Cracking Proceeding of the Corrosion Cracking Program and Related Paper Presented at the International Conference and Exposition on Fatigue, Corrosion, Cracking, Fracture Mechanics and Failure Analysis Organized by American Society for Metals, 1.

Yokobori, A.T.Jr., T. Yokobori, T. Kosumi and N. Takasu (1986). Transactions of the Japan Society of Mechanical Engineers, Vol.53, 1222 (in Japanese).

Table 1. Young's Modulus Measured by Resonance Vibration Test Method

	Young's modulus ($\times 10^5$ MPa)	Standard deviation ($\times 10^5$ MPa)
SiC	3.270	0.208
Alumina	2.262	0.004

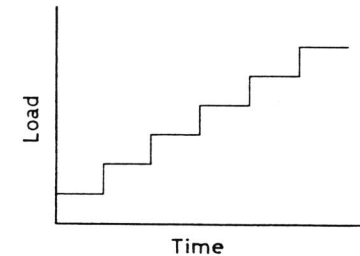
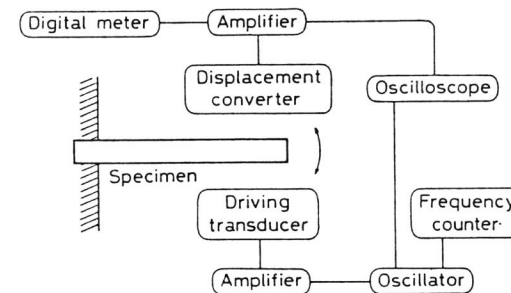


Fig. 1. Quasi Static Loading Test Method

Fig. 2. Block Diagram of Resonance Vibration Test Method for Measurement of Young's Modulus

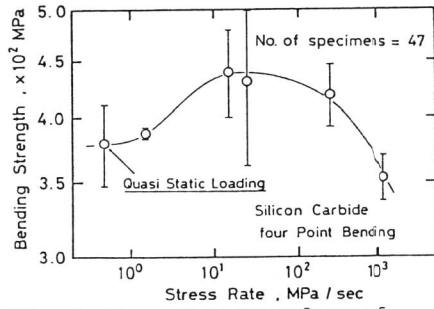


Fig. 3. Stress Rate Dependence of Bending Strength for Silicon Carbide

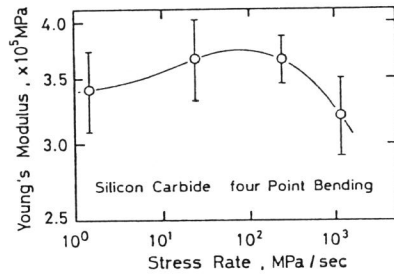


Fig. 4. Stress Rate Dependence of Young's Modulus for Silicon Carbide

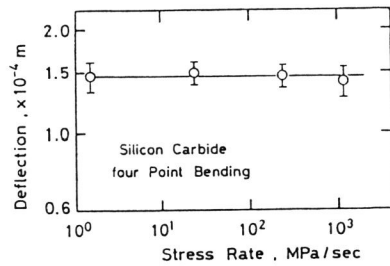


Fig. 5. Stress Rate Dependence of Fracture Deflection for Silicon Carbide

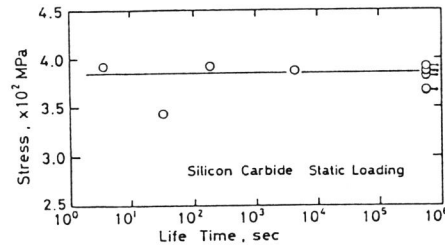


Fig. 6. Static Fatigue Characteristics for Silicon Carbide

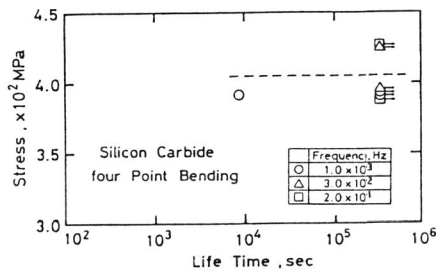


Fig. 7. Cyclic Fatigue Characteristics for Silicon Carbide

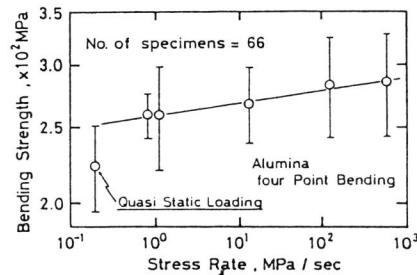


Fig. 8. Stress Rate Dependence of Bending Strength for Alumina Ceramics

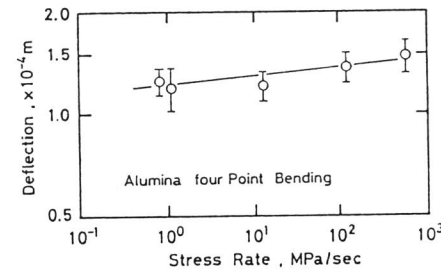


Fig. 9. Stress Rate Dependence of Fracture Deflection for Alumina Ceramics

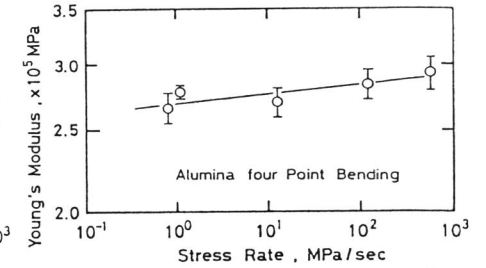


Fig. 10. Stress Rate Dependence of Young's Modulus for Alumina Ceramics

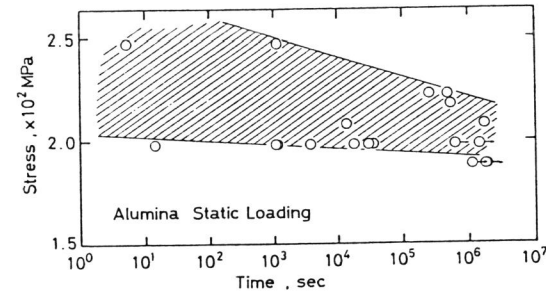


Fig. 11. Static Fatigue Characteristics for Alumina Ceramics

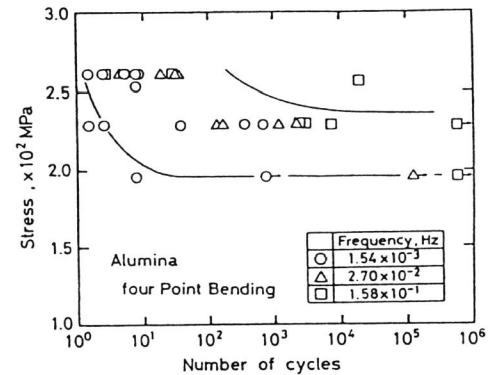


Fig. 12. Cyclic Fatigue Characteristics for Alumina Ceramics

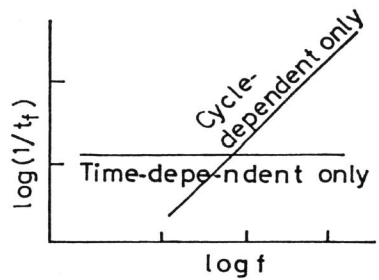


Fig. 13. Representation Method of Time-dependent Mechanism and Cycle-dependent Mechanism for Fatigue Life against Frequency

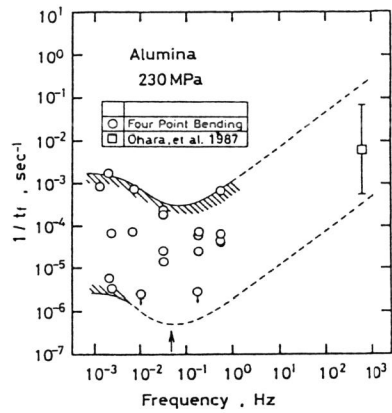


Fig. 14. Frequency Dependence of Fatigue Life of Alumina Ceramics (Stress Amplitude 230MPa)

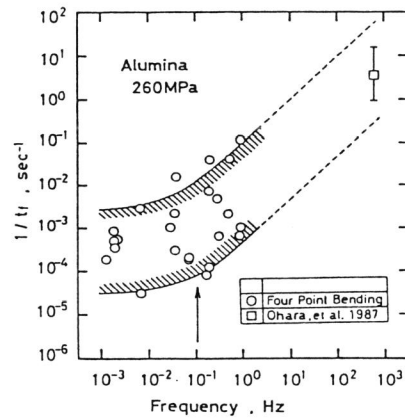


Fig. 15. Frequency Dependence of Fatigue Life of Alumina Ceramics (Stress Amplitude 260MPa)

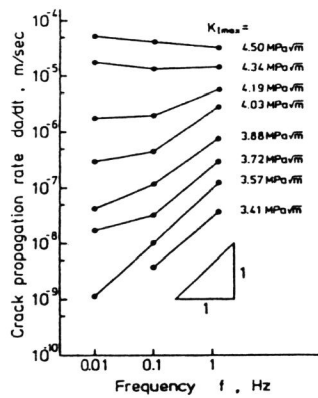


Fig. 16. Frequency Dependence of Crack Propagation Rate of Sintered Silicon Nitride (Kishimoto, et al. 1987)